

Elastic properties of potential superhard phases of RuO₂

J. S. Tse, D. D. Klug, K. Uehara, and Z. Q. Li

Steacie Institute for Molecular Sciences, National Research Council of Canada, Ottawa, Ontario, Canada K1A 0R6

J. Haines and J. M. Léger

Centre National de la Recherche Scientifique, Laboratoire de Physico-Chimie des Matériaux, 1, Place A. Briand, 92190 Meudon, France

(Received 5 November 1999)

First-principles plane-wave pseudopotential and full-potential linearized-augmented plane-wave methods have been used to study the elastic and electronic properties of several potential superhard RuO₂ phases. The structures, relative stabilities, and the elastic constants and bulk moduli of these phases have been calculated within local-density approximation (LDA) and generalized gradient approximation (GGA). In RuO₂, the LDA and GGA approximations yield smaller and larger lattice constants, respectively, for the $Pa\bar{3}$ -RuO₂ structure. The internal structural parameter for oxygen atoms in the $Pa\bar{3}$ structure has a volume dependence that differs from the experimental result and therefore implies a significantly different compression mechanism. The calculated bulk moduli are very similar for the fluorite and $Pa\bar{3}$ structures and therefore apparently independent of the internal structural parameter. The structure and stability of a hypothetical orthorhombic RuO₂ phase is investigated.

I. INTRODUCTION

The search for new superhard materials has been undertaken extensively during recent years¹ and has focused particularly on simple covalent compounds of C, B, and N.²⁻⁴ Recently, a possible new class of hard materials has been suggested: the transition-metal dioxides containing heavy elements.⁵ It has been reported that the bulk modulus of orthorhombic phase of ZrO₂ and CaCl₃-type phase MnO₂ are 332 and 328 GPa, respectively. Furthermore, the bulk modulus of $Pa\bar{3}$ -RuO₂ was found to be 399 GPa,⁶ which is the highest value reported in a material, except for diamond, that has a bulk modulus of 442 GPa. Although hardness is a complex macroscopic property, determined to a large extent by the structure of point defects and dislocations, it is the microstructure, characterized by bond length, bond direction, and atomic size, that determines the ultimate measured strength of a material. For nonmetals, hardness increases with the bulk modulus,⁵ and the bulk modulus is generally higher with smaller bond lengths and strong covalent directional bonds. However, in $Pa\bar{3}$ -RuO₂, the metal-oxygen bond length is 1.99 Å,⁷ which is much longer than that of bond lengths considered up to now as essential in order to have a high bulk modulus. The short bond lengths previously considered required atoms to be small. Understanding the relation between the elastic properties and microstructure of RuO₂ should, therefore, be very helpful in the search for new types of superhard materials.

At ambient pressure, RuO₂ has the rutile ($P4_2/mnm$) structure,^{6,8} and it transforms to a CaCl₂-type ($Pnmm$) structure at about 6 GPa, and then to a cubic fluorite-type structure $Pa\bar{3}$ at above 12 GPa. A detailed study of electronic structure of rutile RuO₂ has been reported by Glassford and Chelikowsky⁹ where it was demonstrated that *ab initio*, local-density methods gave good agreement between calculated density of states and experimental photoemission ex-

periments as well as yielded Fermi surfaces that agree well with experiment. More recently, a full-potential linear muffin-tin orbital (FP-LMTO) calculation on the electronic structure and bulk modulus of cubic-CaF₂($Fm\bar{3}m$)RuO₂ has also been performed by Lundin *et al.*¹⁰ It was suggested that the high-bulk modulus of the cubic form is a result of a strong covalent bonding between ruthenium *d* states and oxygen *p* states. It was shown recently by high-pressure x-ray diffraction and detailed neutron powder diffraction on a quenched sample at 1 bar that the cubic phase is a $Pa\bar{3}$ modified fluorite structure rather than the fluorite ($Fm\bar{3}m$) form.^{6,7}

In this paper, first-principles plane-wave (PW) pseudopotential and full-potential linearized-augmented plane-wave (FLAPW) methods are used to investigate the atomic and electronic structure, bulk modulus, elastic constants, and phase transition pressures in RuO₂ oxide phases.

II. THEORETICAL METHODS

Plane-wave total electronic energy calculations have been performed with the VASP code. A detailed description of VASP and its algorithms can be found in Refs. 11 and 12. VASP is a first-principles plane-wave code based on the density-functional theory that employs the ultrasoft Vanderbilt pseudopotential.¹³ For the calculation of the ultrasoft pseudopotentials, the atomic cutoff radii is 2.65 a.u. for Ru atoms and 1.5 a.u. for O atoms. The atomic configurations are $d^7s^1p^0f^0$ for Ru and $s^2p^4d^0$ for O. The solution of the generalized Kohn-Sham equations is performed using an efficient iterative matrix-diagonalization routine based on a sequential band-by-band residuum minimization method—direct inversion in the iterative subspace. Alternatively, a matrix diagonalization based on a preconditioned band-by-band conjugate gradient algorithm can be used. The charge density is updated using an improved Pulay mixing. For ac-

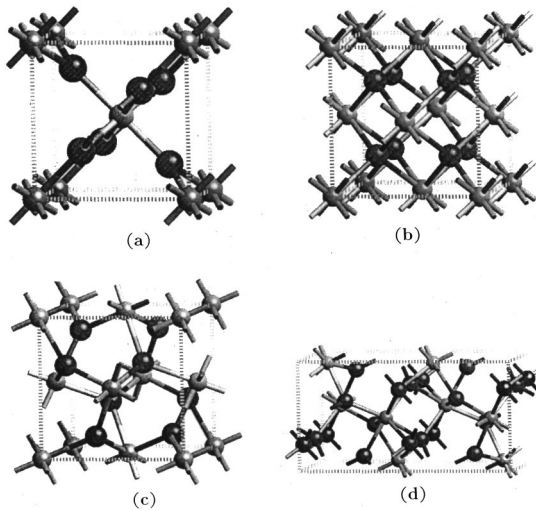


FIG. 1. Structures of the (a) rutile, (b) fluorite, (c) $Pa\bar{3}$, and (d) the hypothetical $Pbcu$ phase of RuO_2 .

curate converged structure optimizations, an energy cutoff of 600 eV was used, and a $12 \times 12 \times 12$ Monkhorst-Pack¹⁴ grid for the k point mesh was employed.

FLAPW calculations have been performed with the WIEN97 program.¹⁵ In this all-electron method, the potential inside the atomic sphere is represented by a linear combination of products of radial functions with spherical harmonics. In the interstitial region between the spheres centered on each atom a plane-wave expansion is used. The solutions to the Kohn-Sham equations are expanded in this compound basis set. The zone integration has been carefully tested to obtain well-converged total energy.

Both the local-density approximation (LDA) and the generalized gradient approximation (GGA) have been used to determine the effect of density gradient corrections on the calculated properties. For LDA, the exchange-correlation functional of Ceperley and Alder as parametrized by Perdew and Zunger was used.¹⁶ For GGA in the plane-wave calculations, the Perdew-Wang¹⁷ functional was used. The Perdew, Burke, and Ernzerhof form¹⁸ of the GGA was used in the FLAPW calculations.

III. RESULTS AND DISCUSSION

Five phases of RuO_2 have been studied here: tetragonal rutile ($P4_2/mnm$), the $CaCl_2$ ($Pnmm$), the cubic modified fluorite ($Pa\bar{3}$), the hypothetical cubic fluorite ($Fm\bar{3}m$) structures, and a potentially stable orthorhombic structure found in other oxides.¹⁹ Figure 1 shows the structure of these four phases (the $CaCl_2$ structure is just an orthorhombic distortion of the rutile structure). In rutile structure, the two Ru atoms occupy $(0, 0, 0)$ and $(\frac{1}{2}, \frac{1}{2}, \frac{1}{2})$ sites while four O atoms occupy $(u, u, 0)$ and $\pm(u + \frac{1}{2}, \frac{1}{2} - u, \frac{1}{2})$ sites, where u is an internal parameter. In cubic fluorite structure, Ru atoms occupy $(0, 0, 0)$ positions, while O atoms occupy $\pm(u, u, u)$ positions, where the internal parameter $u = 0.25$. In the modified fluorite structure ($Pa\bar{3}$), oxygen atoms deviate from their position in fluorite, $u = 0.344$. All structure parameters have been optimized by the plane-wave method and several parameters including the lattice parameters and bulk moduli

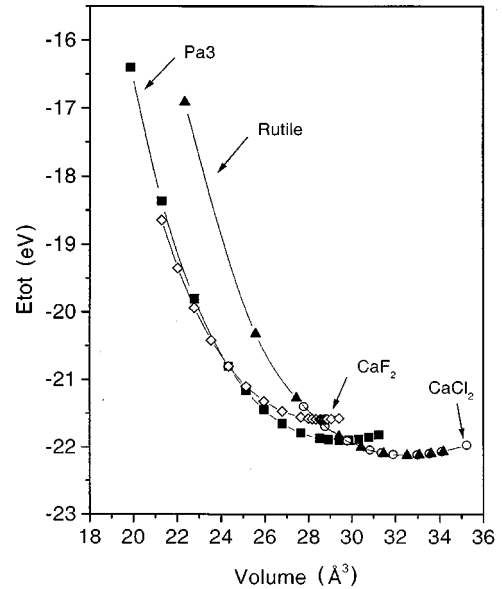


FIG. 2. Calculated energy versus volume for the rutile, fluorite, $CaCl_2$, and $Pa\bar{3}$ phases of RuO_2 obtained with the pseudopotential plane-wave method.

of the cubic phases, as well as the internal structural parameter in the $Pa\bar{3}$ structure, have been confirmed by FLAPW calculations. The structural parameters obtained with the two methods agree within 1% and the bulk moduli agree within 2%. The energy-volume relations calculated with the plane-wave method are shown in Fig. 2. The energy and volume are given per RuO_2 molecule. The results are fit to the first-order Murnaghan equation of state.²⁰ The calculations indicate that the rutile and $CaCl_2$ phases have higher cohesive energy and larger volume than the other phases, and as the pressure increases, the rutile form of RuO_2 transforms first to the $CaCl_2$ form at about 9 GPa, and then to a modified fluorite structure at 13 GPa and to fluorite at 89 GPa. The calculated phase transition sequence and transition pressure for the first two observed transformations using the plane-wave method are in good agreement with experiments,^{6,8,21} see Table I. The calculated transition pressure and therefore the phase stability ordering using the FLAPW method for the $Pa\bar{3}$ to fluorite transition is also in good agreement with the plane-wave results.

The structural parameters calculated at 1 bar with the plane-wave method are listed in Table II along with the available experimental results for comparison. The calculated lattice parameters are in agreement with the experiment to within 2%. The LDA approximation generally underestimates the lattice constant while the GGA approximation

TABLE I. Phase transition pressures of RuO_2 , units: GPa.

	Theory	Experiment
Rutile \rightarrow $CaCl_2$	9	6 ^a , 11.8 ^b
$CaCl_2 \rightarrow Pa\bar{3}$	13	12
$Pa\bar{3} \rightarrow$ Fluorite	89 (97) ^c	

^aReference 8.

^bReference 21.

^cValue in parentheses from FLAPW.

TABLE II. Ambient pressure structure parameters of RuO₂ phases.

	a (Å)			c (Å)			u (Å)		
	LDA	GGA	Expt.	LDA	GGA	Expt.	LDA	GGA	Expt.
Rutile	4.474	4.554	4.493 07 ^a	3.092	3.137	3.106 39	0.3058	0.3054	0.3056
Fluorite	4.743	4.842							
$Pa\bar{3}$	4.792	4.884	4.858 92 ^b				0.3525	0.3503	0.351 15

^aFrom Ref. 25.^bFrom Ref. 7.

overestimates the lattice constants when compared with experiment. This is similar to the results reported for SiO₂.²² The LDA and GGA results for the structural parameters of RuO₂ agree with the experimental data to within 2% (Table II). The bulk moduli and their pressure derivatives were obtained from the Murnaghan equation-of-state fit to the plane-wave results, and are listed in Table III. Two sets of bulk moduli B_0 and its pressure derivative B'_0 with different fitting methods are listed, one with B'_0 fixed at 3.5, as was used in fitting the original experimental results;⁸ the other fit was obtained allowing the B'_0 to vary. The bulk modulus B_0 is sensitive to the choice of B'_0 . If B'_0 is fixed at 3.5, a higher bulk modulus $B_0=380$ GPa is obtained for $Pa\bar{3}$, very close to the experimental value of 399 GPa, which is only 10% smaller than that of diamond. However, if B'_0 is allowed to vary, a smaller value of 346 GPa is calculated. An approximately 10% variation in the bulk modulus can be obtained by these different fitting procedures. Lundin *et al.*¹⁰ have reported the bulk modulus of RuO₂ in CaF₂ structure of 343 GPa obtained with a FP-LMTO method. In this calculation, B'_0 was not fixed. This is in excellent agreement with the value of 351 GPa obtained with a plane-wave pseudopotential LDA calculation where data were fit to the Murnaghan equation-of-state allowing B_0 and B'_0 to vary.

LDA and GGA approximations lead to bulk moduli that differ by up to 15%, see Table III, and GGA in the present calculations often yields values closer to the experiment. This is in agreement with previous calculations on SiO₂ that report that the GGA approximation overestimates the lattice constants, but may overestimate or underestimate the bulk modulus.²² The performance of various density functionals for the exchange-correlation energy has been a subject of considerable interest in the recent literature.^{22,23} For SiO₂,^{22,23} the local-density approximation consistently yields a bulk modulus that is lower than experiment in four-

coordinated α quartz whereas gradient-corrected exchange-correlation energy approximations overestimate the bulk modulus. For six-coordinated stishovite, on the other hand, both local-density and gradient-corrected calculations underestimate the bulk modulus and their magnitudes are in reverse order from that found for α -quartz. Therefore, there is no clear trend for the oxides at present.

As was concluded above, cubic RuO₂ has a very high-bulk modulus, and therefore could be considered as a candidate for a superhard material. However, a high-bulk modulus by itself does not directly imply high hardness. Hardness is related to a number of properties including linear compressibility and shear strength. A fundamental condition for high hardness is that a stress in a given direction should not be transmitted along a different direction, and therefore the shear moduli must also be high. We have, therefore, also calculated the elastic constants of these materials.

The standard method used to calculate elastic constants from *ab initio* results is to determine the second derivatives of the energy density $U(\delta)$ as a function of properly chosen lattice distortions δ that describe the strain.²⁴ For a cubic-crystal structure there are only three independent elastic constants C_{11} , C_{12} , and C_{44} . By application of three independent types of volume compression ϵ_{comp} , tetragonal ϵ_{tetr} , and trigonal ϵ_{trig} lattice distortions, the elastic constants can be obtained as

$$\frac{\Delta^2 U(\epsilon_{\text{comp}})}{\Delta \delta^2} = (C_{11} + C_{12})/3 = B_0, \quad (1)$$

$$\frac{\Delta^2 U(\epsilon_{\text{tetr}})}{\Delta \delta^2} = 2(C_{11} - C_{12})/3, \quad (2)$$

$$\frac{\Delta^2 U(\epsilon_{\text{trig}})}{\Delta \delta^2} = 4C_{44}. \quad (3)$$

The elastic constants of RuO₂ in $Pa\bar{3}$ and fluorite phases have been calculated, and the results are listed in Table IV.

TABLE IV. Elastic constants (in GPa) of RuO₂ in $Pa\bar{3}$ and fluorite structures, compared with that of diamond (Ref. 27).

	$Pa\bar{3}$	Fluorite	Diamond
C_{11}	450	435	1020
C_{12}	189	227	133
C_{44}	147	152	553
G	140	133	509

TABLE III. Bulk modulus (in GPa) of RuO₂ in rutile, fluorite, and modified fluorite structures.

	$B_0(B'_0=3.5)$		$B_0(B'_0)$ Expt.	$B_0(B'_0)$	
	LDA	GGA		LDA	GGA
Rutile	313	260.5	270 ^a (4.0)	299 (4.0)	249 (4.3)
Fluorite	384	336		351 (4.2)	297 (4.1)
$Pa\bar{3}$	380	334	399 ^b (3.5)	346 (4.2)	299 (3.9)

^aFrom Ref. 26.^bFrom Ref. 6.

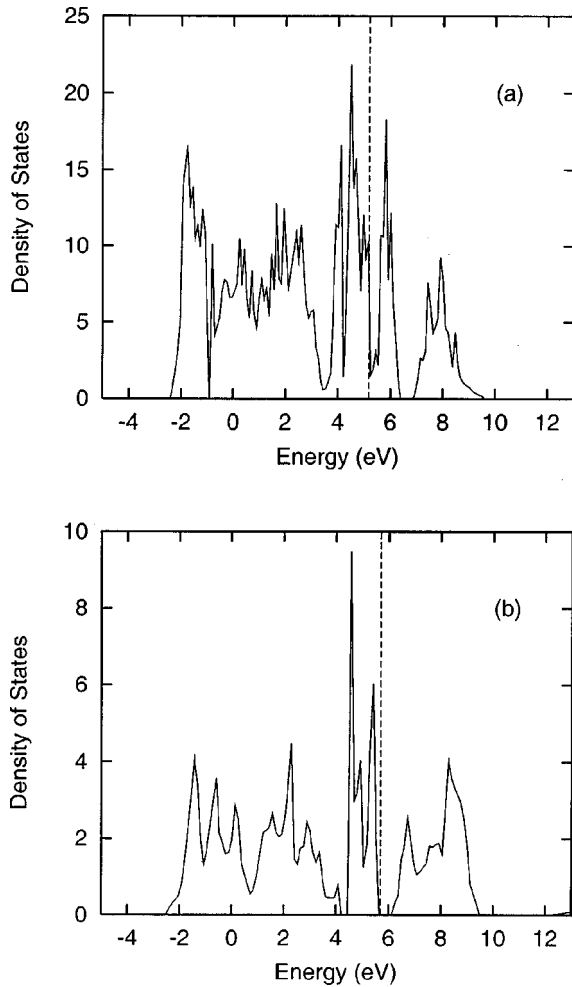


FIG. 3. PW calculated electronic density of states for the (a) $Pa\bar{3}$ and (b) fluorite structures of RuO_2 .

The Voigt-averaged shear modulus $(3C_{44} + C_{11} - C_{12})/5$ is also listed for these phases. Although cubic RuO_2 has a high bulk modulus, its shear modulus is calculated to be smaller than that of diamond.

In order to understand the microscopic mechanism of the high bulk modulus of RuO_2 we have analyzed the electronic structures of the $Pa\bar{3}$ and CaF_2 structures and the density-of-states (DOS) pictures are shown in Fig. 3. The DOS of CaF_2 structure is very similar to the result of Lundin *et al.*¹⁰ obtained by a full potential LMTO method. The spectrum can be divided into four parts; the lowest two parts are primarily due to the bonding and antibonding between O atoms, while the upper two parts are due to the bonding and antibonding of Ru d and O p states. In CaF_2 structure, the bonding and antibonding splitting is very clear, see Fig. 3, leading to a semiconductor with a band gap of about 0.5 eV. In the $Pa\bar{3}$ structure, the Ru atoms are octahedrally coordinated, and therefore the fivefold-degenerate d states split into the triply degenerate t_{2g} and doubly degenerate e_g states. In the $Pa\bar{3}$ space group, distortions away from perfect O_h symmetry lower the metal-atom site symmetry, resulting in further splitting of these states. As a result, the Fermi energy is near the minimum of the t_{2g} manifold, showing a weak metallic feature. The metallic character of the $Pa\bar{3}$ phase is also

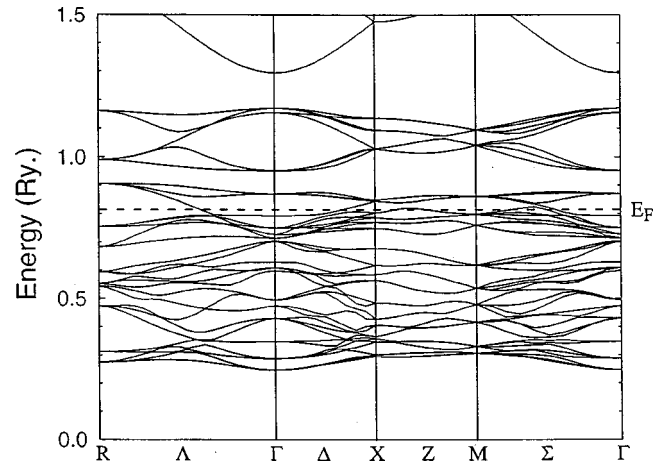


FIG. 4. Calculated band structure for the $Pa\bar{3}$ phase of RuO_2 . The calculated band structure was obtained by the FLAPW method using the GGA approximation. The lattice parameter used in the calculation was 4.90 Å.

clearly reflected in the band structure as shown in Fig. 4. The weak metallic nature of the $Pa\bar{3}$ enabled the acquisition of the Raman spectrum of this phase.⁷

The structural difference between the $Pa\bar{3}$ and CaF_2 phases can be characterized by the internal parameter u , in $Pa\bar{3}$ $u=0.35115$ instead of $u=0.25$ in CaF_2 structure. The displacement of oxygen atoms distorts the coordination polyhedron from cubic to regular rhombohedral, yielding a Ru coordination number of six plus two instead of eight, and leads to a very short O-O distance of 2.5054 Å between rhombohedra along a diagonal of the unit cell; this compares with the corresponding distance in a CaF_2 structure of 4.207 Å. Due to this small O-O distance along the diagonal of the unit cell, there is no empty site at the center of the cell; this makes the $Pa\bar{3}$ structure a better candidate for hard materials.

The study of structural phase transitions in AX_2 compounds has led to suggested pathways among these materials with increasing coordination numbers for the central cation as pressure is increased.¹⁹ One of the most likely pathways, in analogy with other oxides,¹⁹ would indicate that the $Pa\bar{3}$ structure may transform to an orthorhombic $Pbca$ structure. This structure would have a coordination number of 7. To investigate the possibility that this material could be prepared, we calculated the optimized, minimum energy structure of a $Pbca$ phase of RuO_2 at several volumes in order to determine if the structure is stable and to predict the bulk modulus and transformation pressure. These calculations indicated, however, that large forces were always present on the atoms and the structure would not be maintained in particular at high pressures. These results, therefore, predict that the ideal $Pbca$ structure found in ZrO_2 and HfO_2 structures is probably not stable. It would, therefore, be of interest to explore experimentally the structural stability of the $Pa\bar{3}$ phase at high pressures to test this result and to determine the stable post- $Pbca$ structure of RuO_2 .

A particularly sensitive test of the theoretical methods is to determine the effect of pressure on the positional coordinate u of the oxygen atoms in the $Pa\bar{3}$ structure of RuO_2 .

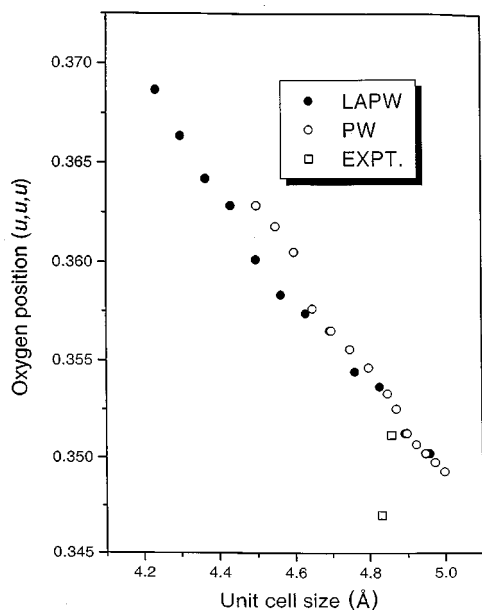


FIG. 5. Experimental and calculated volume dependence of the oxygen structural parameter for the $Pa\bar{3}$ phase of RuO_2 . The calculated points were obtained with GGA.

This positional coordinate defines the site (u, u, u) for atoms on Wyckoff sites $8c$. Experimental studies have found that the u parameter of $Pa\bar{3}RuO_2$ decreases with increasing pressure.^{6,7} The present calculations using PW and FLAPW methods on the relation of u to pressure indicate that u increases with increasing pressure and consequently, the shortest O-O distances between polyhedra shorten (Fig. 5). A search for the possibility of two or more minimum-energy structures and optimum u parameter was performed and only one minimum-energy solution was found. The volume dependence of u was nearly independent of whether the GGA or LDA approximations were used in the LAPW or plane-wave pseudopotential calculations. For example, points calculated with the LDA approximation in the FLAPW method gave the same slope and the u values were very slightly lower and within 0.003 of the GGA values shown in Fig. 5. The calculated value for u is in excellent agreement with the experimental value for samples recovered at 1 bar pressure. The main source of uncertainty in the experimentally determined u parameter at high pressure is the presence of some untransformed lower-pressure phase, for which some lines overlap those of the cubic phase.

The calculated O-O distances, corresponding to the 1 bar lattice constant, for the edges and face diagonals of the rhombohedron centered about the Ru cation, are 2.625 and 2.992 Å, which also compare very well with the experimentally determined values of 2.6208 and 2.9935 Å, respectively. We have calculated the diffraction patterns for the different values of u at the lattice constants determined by experiment and compare them with the diffraction patterns that would be obtained with the values of u predicted at these lattice parameters by the theoretical results in Fig. 6. It is clear that at ambient pressure the diffraction patterns are essentially identical. At a pressure of 8.9 GPa, there is a difference between theory and experiment that should be above experimental accuracy. The largest difference is in the (200)

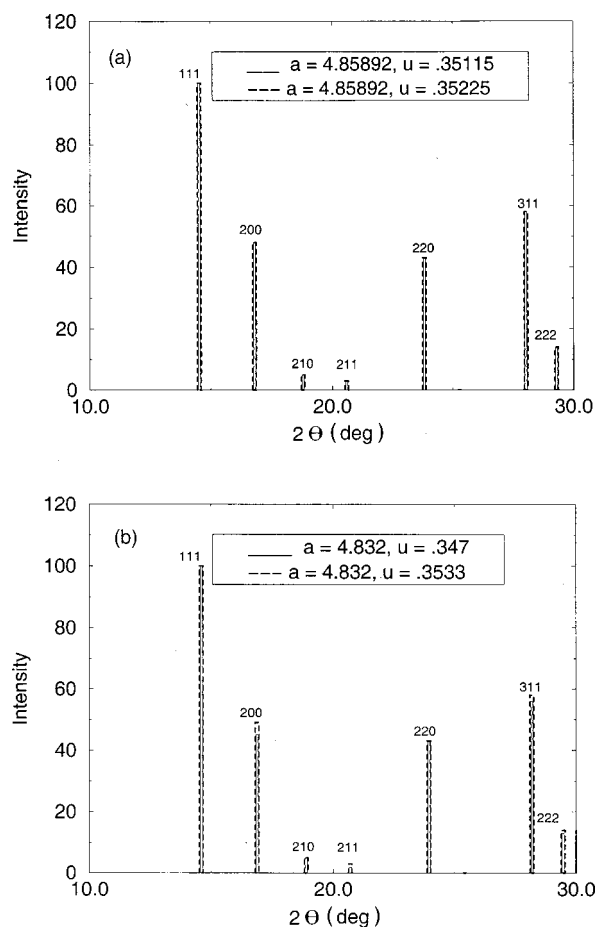


FIG. 6. Simulated x-ray diffraction patterns for the $Pa\bar{3}$ phase with the calculated and experimental structural parameter for oxygen at 1 bar (a) and 8.9 GPa (b). The calculated diffraction patterns are for a randomly oriented polycrystalline sample using a Mo 0.709 319-Å x-ray source. In the top frame the calculated diffraction patterns for the experimentally determined structure and for the optimized calculated structure with the same lattice constant $a = 4.85892$ Å using the LAPW method are shown. The diffraction patterns in the lower frame are obtained using the experimental lattice constant at 8.9 GPa.

reflection and there was no indication in the experiment of splitting in this peak that may be caused by nonhydrostatic conditions. Defects are also not thought to be important in this material. The calculated increase in u with increasing pressure implies that the rhombohedral coordination polyhedra consisting of a Ru^{4+} surrounded by eight O^{2-} ions with a coordination number of 6 + 2 in the structure would have a similar compressibility as the unit cell, which is in contrast to the trend suggested by the limited experimental results. This would have important implications for the mechanism of compressibility in these and related materials.⁷ Although it appears that discrete fourier transform theory is sufficiently accurate to determine the u parameter in this structure, this discrepancy needs to be resolved since this system provides a sensitive test for the theoretical methods. Clearly further work is required to understand the origin of the different experimental and theoretical results.

In summary we report a study of the electronic structures, structural parameters, and elastic properties of four phases of RuO_2 employing plane-wave and FLAPW methods. The re-

sults have shown that the $Pa\bar{3}$ structure of RuO_2 has a calculated bulk modulus within 5–10% of the experimentally determined result. This is close to that of diamond, which is the hardest material known at present. The detailed comparison of the theoretical methods with the experimental results further demonstrates that the LDA and GGA approximations yield values for structural parameters that bracket the experimental values as has been found in SiO_2 . A hypothetical $Pbca$ structure has been investigated and it is calculated to be unstable. It is found that the oxygen structural parameter u in

the $Pa\bar{3}$ and fluorite phases is significantly different although the bulk moduli for these materials are similar. This has important implications for the compression mechanism in these materials and it would be of interest to explore this in other oxides.

ACKNOWLEDGMENT

We thank Dr. R. Rousseau for very helpful discussions.

-
- ¹J. M. Léger and J. Haines, *Endeavour* **27**, 121 (1997).
²M. L. Cohen, *Science* **261**, 307 (1996).
³R. Riedel, *Adv. Mater.* **4**, 759 (1992).
⁴D. M. Teter and R. J. Hemley, *Science* **271**, 53 (1996).
⁵J. M. Leger, J. Haines, and B. Blanzat, *J. Mater. Sci. Lett.* **13**, 1688 (1994).
⁶J. Haines, J. M. Léger, and O. Shulte, *Science* **271**, 629 (1996).
⁷J. Haines, J. M. Léger, M. W. Schmidt, J. P. Petitet, A. S. Pereira, J. A. H. Jornada, and S. Hull, *J. Phys. Chem. Solids* **59**, 239 (1998).
⁸J. Haines and J. M. Léger, *Phys. Rev. B* **48**, 13 344 (1993).
⁹K. M. Glassford and J. R. Chelikowsky, *Phys. Rev. B* **47**, 1732 (1993).
¹⁰U. Lundin, L. Fast, L. Nordstrom, B. Johansson, J. M. Wills, and O. Eriksson, *Phys. Rev. B* **57**, 4979 (1998).
¹¹G. Kresse and J. Furthmuller, *Phys. Rev. B* **54**, 11 169 (1996); *Comput. Mater. Sci.* **6**, 15 (1996).
¹²G. Kresse and J. Hafner, *J. Phys.: Condens. Matter* **6**, 8245 (1994).
¹³D. Vanderbilt, *Phys. Rev. B* **41**, 7892 (1990).
¹⁴H. Monkhorst and J. Pack, *Phys. Rev. B* **13**, 5188 (1976).
¹⁵P. Blaha, K. Schwarz, and J. Luitz, WIEN97, *A Full Potential Linearized Augmented Plane Wave Package for Calculating Crystal Properties* (Technical University Wien, Vienna, 1999).
¹⁶J. P. Perdew and A. Zunger, *Phys. Rev. B* **23**, 5048 (1981).
¹⁷J. Perdew, in *Electronic Structure in Solids '91*, edited by P. Ziesche and H. Eschrig (Akademie Verlag, Berlin, 1991).
¹⁸J. Perdew, K. Burke, and M. Ernzerhof, *Phys. Rev. Lett.* **77**, 3865 (1996).
¹⁹J. M. Léger and J. Haines, *Eur. J. Solid State Inorg. Chem.* **34**, 785 (1997).
²⁰F. Birch, *J. Geophys. Res.* **57**, 227 (1952).
²¹S. S. Rosenblum, W. H. Weber, and B. L. Chamberland, *Phys. Rev. B* **56**, 529 (1997).
²²A. Zupan, P. Blaha, K. Schwarz, and J. P. Perdew, *Phys. Rev. B* **58**, 11 266 (1998).
²³D. R. Hamann, *Phys. Rev. Lett.* **76**, 660 (1996).
²⁴M. J. Mehl, J. E. Osburn, D. A. Papaconstantopoulos, and B. M. Klein, *Phys. Rev. B* **41**, 10 311 (1990).
²⁵J. Haines, J. M. Léger, O. Schulte, and S. Hull, *Acta Crystallogr., Sect. B: Struct. Sci.* **53**, 880 (1997).
²⁶R. M. Hazen and L. W. Finger, *J. Phys. Chem. Solids* **42**, 143 (1981).
²⁷*The Properties of Diamond*, edited by J. E. Field (Academic, New York, 1979).